JOURNAL OF CATALYSIS 30, 195–203 (1973)

Studies of Molybdena–Alumina Catalysts

I. The Formation of Mo(V) in Reduced MoO_3–Al_2O_3 Systems and the Determination of Its Absolute Concentration by ESR Techniques

K. S. SESHADRI AND L. PETRAKIS*

Gulf Research and Development Company, Pittsburgh, Pennsylvania 15230

Received December 19, 1972

The formation of Mo(V) was studied in the hydrogen reduced MoO_3–Al_2O_3 system at different times and temperatures of reduction (by observing its electron spin resonance signal). The necessary computational procedure and appropriate standards were developed to measure the absolute concentration of Mo(V) in these samples. The ESR signal intensity increased rapidly with time of reduction, attained a maximum, then decayed and reached a plateau with continued reduction. Increase in reduction temperature decreased the amount of Mo(V) formed, and the maximum occurred at shorter reduction times. The spectra were interpreted in terms of Mo(V) occupying axially symmetric sites and the observed g-values indicate that Mo(V) is in slightly different environments in η- and γ-Al_2O_3.

INTRODUCTION

Hydrodesulfurization (HDS) of fossil fuels has become recently increasingly important. Typically, the process uses a catalyst, the major component of which is molybdenum and promoters such as cobalt or nickel supported on active alumina. The overall HDS reaction is complex, but, considering the molybdenum only, it is known that this active component is reduced to lower valence states and is also sulfided during the process. The active sites at which the HDS reaction takes place have been the subject of several investigations (*1*). A detailed study of the reduction of molybdena–alumina was undertaken to better define the overall role of its surface structure and the phases produced during reduction and/or sulfiding in the HDS process.

Supported hexavalent molybdenum is reduced to lower valence states, including the pentavalent state, by hydrogen, hydrocarbons, and hydrogen and hydrogen sulfide mixtures, while in the reduced unsupported molybdenum oxide no pentavalent state has been detected. This information has been provided by electron spin resonance study of these systems (*2*). Both penta- and tetravalent molybdenum species are paramagnetic; but the ESR signal due to Mo(IV) is hard to detect at room temperature, whereas the resonance absorption due to Mo(V), in a suitable environment, is readily observable even at room temperature. In addition to identifying the Mo(V), the spin resonance spectra can give information concerning the bonding and the environment of the molybdenum oxide. Extensive investigation (*3*) of the bonding in halogen complexes of Mo(V) by a study of their spin resonance and electronic spectra has been made. By careful measurement of g-values, information on the crystal field can be obtained. It is also possible to measure the absolute concentration of Mo(V) formed. These kinds of information, when combined with additional data from other techniques, can hopefully provide a better insight into the behavior of molybdena–alumina catalysts.

The present work was undertaken with three aims in mind: (1) to follow the con-

---

* To whom inquiries should be addressed.

centration of Mo(V) with different time and temperature of reduction, (2) to relate certain spectral parameters to the environment of Mo(V) in aluminas, and (3) to develop appropriate standards and a procedure to measure the absolute concentration of Mo(V) in the reduced MoO_3-η- and γ-Al_2O_3. In connection with this last point and because of the uncertainties that often plague determination of absolute concentrations, we have chosen to make a detailed investigation of the applicability of the ESR to the determination of absolute Mo(V) concentration. Of course, the technique is more widely applicable to other systems containing transition metal ions.

EXPERIMENTAL

The catalysts used in this investigation were prepared by wetting the support (η- and γ-Al_2O_3) with an aqueous solution of ammonium paramolybdate to give 10% by weight Mo in the final sample. Impregnation was followed by drying at 100°C for 2 hr. Subsequently, it was heated in a stream of dry air at 500°C for nearly 18 hr. Then 0.5 g of the material in 20–40 mesh pellet form was loaded into a Pyrex glass reactor and heated to the required temperature in helium; then helium was replaced by hydrogen. After passing hydrogen for the required time, the reduced sample was cooled in helium to room temperature, evacuated for about 15 min, and the sample transferred to a side ESR tube to a height of 10 cm and sealed. The heating and cooling periods were 15 min. Reduction was at temperatures 300, 400, 500, and 750°C with reduction times of 5, 15, 25, 35, and 120 min. A quartz reactor was used for the 750°C reduction. During the entire operation, care was taken to rigorously exclude air.

The ESR measurements were made with a Varian V-4500 *x*-band spectrometer equipped with a 9- or 12-in. magnet, a "Fieldial", NMR gaussmeter, and a 100-kHz modulation unit. A solution of DPPH in benzene ($g = 2.0035$) served as calibration standard in g-value measurements. Intensity measurements were made using a dual sample cavity, one channel modulated at 100 kHz and the other at 400 Hz. The spectra on chart were converted to digital form on a CALMA digitizer and double-integrated to obtain the area under the zero derivative curve, using a computer program. The program utilizes a gaussian quadrature formula for the first integration and Simpson's one-third rule for the subsequent integration.

The standards for ESR intensity measurement were chosen with particular care. A transition metal ion, which can be easily and accurately analyzed by gravimetric methods that is evenly distributed in a support similar to that used in catalyst preparation, can be an appropriate standard. Cu(II) in Y-type Na^+ zeolite and Cu(II)–Al_2O_3 were the two standards tested. Supported hydrated Cu(II) gives broad single-line absorption (*4*), and there are excellent wet chemical methods by which copper can be analyzed. Three samples of Cu(II)–zeolite with different levels of copper were prepared by ion exchange, and in one of them copper was quantitatively analyzed by an electrochemical method. Using this as the standard, copper content in the other two was measured by x-ray fluorescence and also by ESR. Three Cu(II)–Al_2O_3 standards were prepared by stirring Al_2O_3 and $CuSO_4$ solution, followed by filtration and drying of the residue, and the copper content was analyzed by the procedures mentioned above. Also, Cu(II) in zeolite samples was measured by ESR, using one of the Cu–Al_2O_3 standards. Cu(II)–zeolite-(1) standard was used for measuring the spin concentration of Mo(V) in the reduced samples. The cross-checking of the standards and of the computational procedures gave us confidence that a reliable method has been developed for the Mo(V) absolute concentration determination that is more widely applicable to transition metals in catalysts in general.

RESULTS

Quantitative Determination of Samples

We will first consider the procedure for the quantitative determination of Mo(V) in catalytic samples. Quantitative measurements by spectroscopic techniques often employ a comparison method in which the area under the absorption curve of the unknown is compared with that of a standard with known spin concentration. Relating the spin concentration of the standard to the unknown involves the substitution of the standard sample for an unknown sample in the microwave cavity of the spectrometer. In such a procedure, several conditions have to be satisfied (*5*) if reliable results are desired: (1) the filling factor of the standard and unknown must be identical; (2) materials of high dielectric constant are to be avoided; (3) the spin concentration and the signal width of the standard and unknown should be comparable; (4) the RF power used should be such that signals are not saturated; (5) the cavity must be matched to the same degree for each sample; and (6) the crystal leakage must be always adjusted to the same level. Most of these experimental difficulties are overcome by using the dual-sample cavity (*6*), which permits the simultaneous and independent observation of the two signals. When data are available from the standard and unknown in both the channels, the following expression is used to calculate the spin concentration in the unknown (*5*):

$$N_k/N_u = \left\{\frac{M_{k_1}M_{k_2}G_{u_1}G_{u_2}}{M_{u_1}M_{u_2}G_{k_1}G_{k_2}}\right\}^{1/2},$$

where N = number of spins; M = integrated area; G = amplifier gain; k and u subscripts refer to the known standard and unknown, respectively, and 1 and 2 are the two cavities. For the above equation to be applicable, the modulation amplitude in a given channel should remain unchanged for a run. The spin concentrations in the standards [Cu(II)–zeolite and Cu(II)–Al_2O_3] measured by x-ray fluorescence and ESR in the manner just outlined are given in Table 1, while Table 2 gives the spin concentration in Cu(II)–zeolite standards, measured by ESR with Cu–Al_2O_3(A) standard. The agreement is within ±25%, which is really the limit of accuracy. The precision of our measurements, tested separately, is better than ±10%.

TABLE 1

ANALYSIS OF COPPER STANDARDS[a]

	Copper (II) content (spins/g × 10^{-19})			
Standard	Gravimetric	X Ray Fluorescence	ESR	(%) Difference
CuNa-YZ (1)	36.0	—	—	—
CuNa-YZ (2)	—	32.5	37.9	+14
CuNa-YZ (3)	—	24.2	22.6	−6
Cu–Al_2O_3 (A)	17.2	—	—	—
Cu–Al_2O_3 (B)	—	19.1	17.7	−7
Cu–Al_2O_3 (C)	—	23.5	20.4	−13

[a] The gravimetric and X ray fluorescence methods have an accuracy and precision of 0.5%.

ESR Spectra

Representative spectra of reduced MoO_3–Al_2O_3 and evacuated at 500°C for 2 hr are shown in Figs. 1 and 2, respectively. The signal is attributed to Mo(V) in an environment of axial symmetry. When supported on Al_2O_3, hexavalent molybdenum is reduced, to some extent, to the pentavalent state during calcination in air or evacuation at elevated temperatures. The spin concentration in the air-calcined sample is about 10^{17} spins/g and is slightly enhanced in the evacuated sample. The amount of pentavalent molybdenum is about a hundredth of a percent and probably would not affect any bulk properties, such as magnetic susceptibility. Reduction by hydrogen enhances the spin concentration by nearly a factor of about 1000.

TABLE 2

SPIN CONCENTRATION IN Cu-Y ZEOLITE STANDARDS USING Cu–Al_2O_3 (A) AS THE STANDARD

	Copper (II) content (spins/g × 10^{-19})			
	Cu–Al_2O_3 (A) std	Gravimetric	ESR Cu–YZ (1) std	(%) Difference
Cu–YZ (1)	45.9	36.0	—	−21
Cu–YZ (2)	47.7	—	37.9	−20
Cu–YZ (3)	26.5	—	22.6	−15

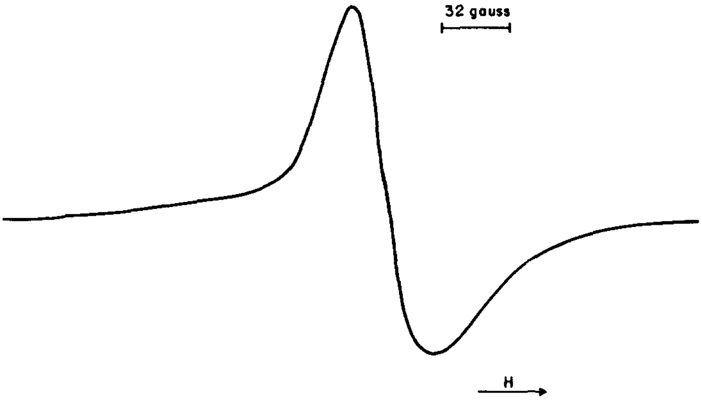

FIG. 1. ESR spectrum of reduced (H_2, 25 min, 300°C) MoO_3-η-Al_2O_3 (10% Mo by wt).

Variation of Mo(V) Signal Intensity with Reduction Time and Temperature

The spin concentrations of Mo(V)/g plotted against time for two (η and γ) aluminas at different temperatures are shown in Fig. 3. Figure 4 shows similar variations on the same support (η-Al_2O_3) at four different temperatures. The results shown in Fig. 3 indicate that there is little difference between the amount of Mo(V) formed in η- and γ-Al_2O_3. But a significant difference exists between η- and γ-Al_2O_3 in the amounts of Mo(V) formed in the air-calcined and high-temperature evacuated sample. The two aluminas have different catalytic activity and behave differently towards the reduction of TCNE to $TCNE^-$ (*7*); η-alumina is more active than γ-Al_2O_3 for the double-bond isomerization of 1-pentene (*8*). It may be expected that this difference will be reflected in the formation of Mo(V) on these two supports. The difference in the high temperature evacuated samples has been attributed by Dufaux *et al.* (*9*) to difference in the basicity of the two supports. Little difference in Mo(V) formation observed between η- and γ-Al_2O_3 on reduction suggests that the reduc-

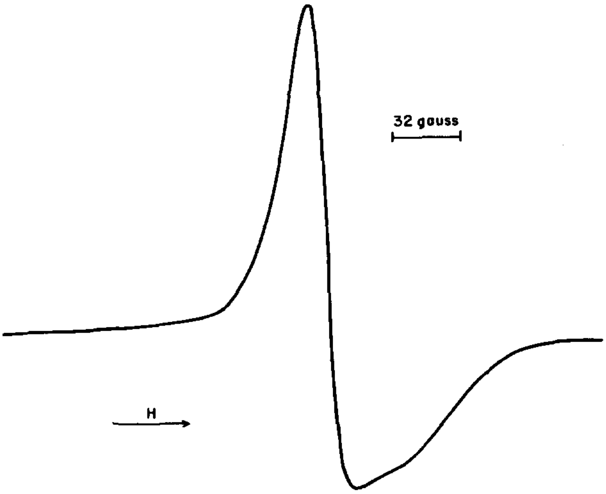

FIG. 2. ESR spectrum of high-temperature evacuated (2 hr, 500°C) MoO_3-η-Al_2O_3 sample (10% Mo by wt).

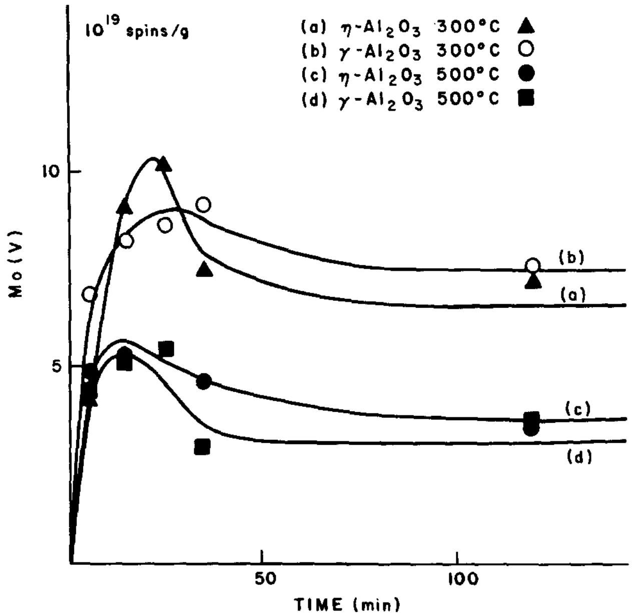

FIG. 3. Variation of Mo(V) concentration in reduced MoO_3-Al_2O_3 (η and γ) with time and temperature.

tion of molybdena in hydrogen to form Mo(V) is not a strong function of the alumina surface.

Concerning the variation of signal intensity with time of reduction, a salient observation is that there is rapid formation of Mo(V) in the first few minutes of reduction, followed by a slower increase to a maximum followed by a decrease, eventually reaching a plateau. This suggests that Mo(V) is an intermediate in the reduction path of Mo(VI) to lower valent Mo states. Our results are similar to those published by Peacock *et al.* (*10*) in their work on oxidation of propene over bismuth molybdate catalysts. Evidently, there are two reactions taking place at different rates, depending on the temperature and duration of reduction. The initial reduction results in the formation of Mo(V), which is then reduced to lower valence states. This explains the rapid increase in Mo(V) concentration, reaching a maximum, and then decreasing with time. However, instead of decaying to zero after the maximum, the signal intensity becomes practically constant with reduction time, showing a residual stable state with continued reduction. As the reduction temperature is increased, the amount of Mo(V) formed decreases, and the maximum occurs at shorter times for higher temperatures. The difference is quite dramatic, the maximum being attained at 750°C almost immediately, while at 300°C the maximum is attained at about 25 min. At elevated temperatures, the further reduction of pentavalent molybdenum to the tetra- and lower valence states is rapid both more and ex-

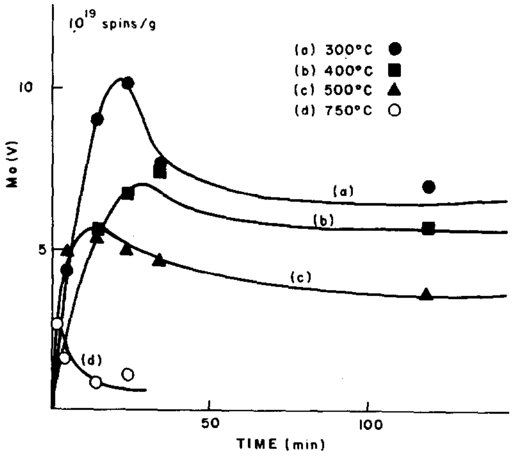

Fig. 4. Variation of Mo(V) concentration in reduced MoO_3–η-Al_2O_3 with time and temperature.

tensive than at lower temperatures, which will account for the decrease in the amount of Mo(V) formed and also the shift in maxima to shorter times.

g-Values of Mo(V)

It has been established that *(2, 9)* the ESR properties of Mo(V) in Al_2O_3 and in other similar supports can be described by the axially symmetric Hamiltonian, in which the hyperfine term, which is applicable to only 25% of the molybdenum isotopes with nonvanishing spin, is neglected,

$$H = \beta_0[g_\parallel H_z S_z + g_\perp(H_x S_x + H_y S_y)],$$

where $g_\parallel$ and $g_\perp$ are the spectroscopic splitting factors, parallel and perpendicular to the symmetry axis; H is the applied field; S the effective spin of the system; and β_0 the Bohr magneton. Since an axial symmetry has been assumed, the spin resonance properties of the ion will depend on the angle between the external magnetic field and its symmetry axis. In polycrystalline material, the ions are randomly oriented, and the observed spectrum will be the sum of the resonances for all orientations. An expression for the intensity distribution can be derived, which is *(11)*

$$S(H) = dN/dH = N_0(4H_0^2/H^3) \times [(g_\parallel{}^2 - g_\perp{}^2)\{(2H_0/H)^2 - g_\perp{}^2\}]^{-1/2},$$

where N_0 is the total number of spins, H and H_0 the values of the magnetic field. $S(H)$ has the properties of Dirac delta function, while the observed spectra have finite width. Mathematically, the observed distribution can be expressed by *(12)*,

$$I(H) = \int_{H_\perp}^{H_\parallel} F(H - H_0)S(H_0)dH_0,$$

where $F(H - H_0)$ is either a Lorentzian or Gaussian function. For weak anisotropy $S(H)_0$ can be replaced by $(H_0 - H_\perp)^{-1/2}$. Hence

$$I(H) = \int_{H_\perp}^{H_\parallel} F(H - H_0)(H_0 - H)^{-1/2}dH_0,$$

which by the following substitutions,

$$\chi = (H - H_\perp)/\Delta H_i;$$
$$\delta = \Delta H_{\text{an}}/\Delta H_i;$$
$$y = (H_0 - H)/\Delta H_i;$$

where $2\Delta H_i$ is the width of the function $F(H - H_0)$ at half the maximum height and $\Delta H_{an} = |H_\parallel - H_\perp|$ can be transformed to

$$I(x) = \int_0^\delta F(x - y)y^{-1/2}dy.$$

Lebedev *(12)* has calculated this function for several values of δ, both for Gaussian and Lorentzian distributions. By comparing the experimental spectra with theoretical spectra in which $F(x - y)$ is Gaussian, we have extracted $g_\perp$ and $g_\parallel$ values. The spectrum of the reduced sample corresponds to the theoretical spectrum with $\delta = 2$, while the spectrum of the high-temperature evacuated samples corresponds to $\delta = 3$. This is to be expected, since ΔH_i is larger in the former than in the latter. The g values are given in Table 3 along with those reported by Burlamacchi *et al.* *(13)* for bismuth molybdate and by Dufaux *et al.* *(9)* for aluminas and for MgO, measured by us earlier.

DISCUSSION

In the reduced MoO_3–Al_2O_3 system, several valence states of Mo are possible; Mo(VI) is nonparamagnetic. Hydrogen-reduced, unsupported MoO_3 has been studied by X ray, and no phase corresponding to the trivalent oxide has been detected *(14)*. Although a similar behavior on the part of supported MoO_3 cannot be expected, no line has been observed in the spin resonance spectra of reduced samples that can be assigned to Mo(III). It has been established that only a minor portion of the total molybdenum is in the pentavalent state; so a significant portion must be present as Mo(IV). Tetravalent molydenum is a d^2 ion and, in its possible environment on Al_2O_3, rather short spin-lattice relaxation times can be expected. This would lead to very broad resonance absorption, which would be unobservable at room and perhaps even at extremely low temperatures. The resonance absorption of Mo(V) is observable at room temperature, when present in an environment of symmetry less than cubic. The hyperfine structure due to the odd isotopes of molybdenum ($I = 5/2$ for

TABLE 3
Spectral Parameters of Mo(V) Signal

Sample	$g_\perp$	$g_\parallel$	Δg	$1/\alpha^c$
Mo–η-Al_2O_3, evacuated 2 hr 500°C	1.9459	1.8942	0.0517	0.522
Mo–γ-Al_2O_3, evacuated 2 hr 500°C	1.9443	1.8896	0.0547	0.603
Mo–η-Al_2O_3, H_2 reduced 500°C 25 min	1.9467	1.8986	0.0481	0.536
Mo–γ-Al_2O_3, H_2 reduced 500°C 25 min	1.9432	1.8998	0.0434	0.576
Mo–η-Al_2O_3, H_2 reduced 300°C 25 min	1.9408	1.8960	0.0448	0.578
Mo–γ-Al_2O_3, H_2 reduced 300°C 25 min	1.9421	1.9000	0.0421	0.588
Mo–MgO, H_2 reduced 490°C 2 hr	1.9386	1.8996	0.0390	0.620
Bismuth molybdate, evacuated at 450°C	1.935	1.872	0.0630	0.508^a
Mo–η-Al_2O_3, evacuated at 600°C (5.4% MoO_3)	1.955	1.912	0.043	0.523^b
Mo–γ-Al_2O_3, evacuated at 600°C (6.5% MoO_3)	1.953	1.922	0.041	0.607^b

[a] Ref. (*13*).
[b] Ref. (*9*).
[c] $1/\alpha = (g_e - g_\perp)/(g_e - g_\parallel)$.

^{95}Mo and ^{97}Mo) was not observed. This is almost certainly due to a large extent to anisotropic effects.

The crystal field in which the transition metal ions reside in catalytic samples and the changes during catalytic reaction have been the subject of many investigations by ESR spectroscopy (*15*). Detailed calculations on Mo(V) in amorphous media have not been attempted. We have analyzed the spectra of Mo(V) in η- and γ-Al_2O_3 and have extracted g values, which give a fairly accurate picture of the environment of the Mo(V) and show a distinction between the two aluminas. Differences in the X ray spectra of η- and γ-Al_2O_3 have been observed (*16*) which agree with our results.

It is accepted that aluminas possess defect spinel structures, with complex surface structures; many crystal planes, edges, or corners may be exposed. X ray diffraction evidence (*15b*) shows that, in γ-Al_2O_3, a considerable part of the surface is formed by the 100 plane of the spinel lattice, which has open octahedral and tetrahedral sites. Sites of lower symmetry are also possible. The spectral features of Mo(V) signal suggest that these ions are occupying the open octahedral sites rather than open tetrahedral sites. The anisotropic spectrum of Cu(II) has been interpreted assuming that these ions are in open octahedral sites (*15b*). The ionic radii of Cu(II) and Mo(V) are comparable, and it is not unreasonable to expect that Mo(V) can also occupy the same site. The five fold degenerate levels of d^1 ion are split into a doubly degenerate (e_g) and a low lying triply degenerate level (t_2g). The levels are further split by tetragonal distortion of the crystal field: e_g to a_{1g} and b_{1g} and t_{2g} to b_{2g} and e_g, which are schematically represented in Fig. 5(a). Figure 5(b) shows the structure of Mo(V)–O complex of C_{4v} symmetry. The tetragonal distortion gives an asymmetric signal with

$$g_\parallel = g_e - (8\lambda/\Delta),$$
$$g_\perp = g_e - (2\lambda/\delta),$$

where $\Delta = E_{b_{1g}} - E_{b_{2g}}$ and $\delta = E_{e_g} - E_{b_{2g}}$.

The expressions for $g_\parallel$ and $g_\perp$ are approximate, because the terms which represent the nature of bonding between the metal and ligand atoms have been neglected. Nevertheless, the quantity

$$1/\alpha = \frac{g_e - g_\perp}{g_e - g_\parallel} = \frac{1}{4}\frac{\Delta}{\delta}$$

has been shown by Dufaux, Che, and Naccache (*9*) to fairly accurately reflect the environment in which Mo(V) is situated. The value of α in γ-Al_2O_3 in the samples which we have studied is con-

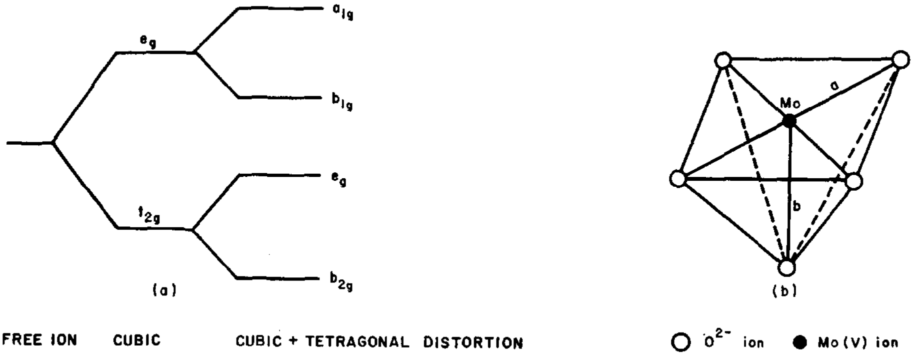

FIG. 5. Energy levels of Mo(V) ion in a cubic and cubic + tetragonal field and the structure of a Mo(V)-oxide.

sistently larger than in η-Al_2O_3. The difference is 13% in the high-temperature evacuated samples, and a similar difference (16%) has been observed by Dufaux *et al.* (*9*). In the reduced samples, the difference is not so marked. A more accurate measurement of $g_\parallel$ and $g_\perp$ is possible in the high-temperature evacuated samples than in the reduced samples, since the lines are narrower and the shoulder corresponding to the position $g_\parallel$ is better resolved. We believe that the structural differences which exist in the high-temperature evacuated samples continue to be present, except that, due to increased concentration of Mo(V), the lines are broadened. The quantity Δ is a function of the equatorial Mo–O distance (a), while δ depends on both the equatorial and Mo–O distance along the C_4 axis (b). Both (a) and (b) or one of them can vary depending on the degree of tetragonal distortion. A distortion, in which the distance along the C_4 axis is elongated and the equatorial distances are shortened, results in a larger value for α; and a smaller value for α would result from an opposite effect. Though these effects are not readily quantified, the results suggest that the amount of tetragonal distortion in η- and γ-Al_2O_3 is not identical, agreeing with the structural difference observed by X ray diffraction studies (*16*). The value of α in bismuth molybdate and in MgO is similar in magnitude to that observed in aluminas. This is to be expected. Since resonance absorption has been observed in all these supports at room temperature, it is reasonable to expect that Mo(V) is in a similar environment, with variations in the degree of tetragonal distortion.

Although a distinct structural difference is observed between the two supports, they favor the formation of Mo(V) to equal extent upon reduction at high temperatures, whereas, in samples evacuated at elevated temperature, more Mo(V) is formed in η-Al_2O_3 than in γ-Al_2O_3. It is likely that this difference is due to the dissimilarity in surface characteristics, and this difference is wiped out to a large extent on hydrogen reduction. Upon hydrogen reduction, there is rapid formation of Mo(V) with time, followed by a slow increase. X ray diffraction fails to detect any crystalline phase of Mo for levels up to 10–15%. Hence, it is reasonable to suppose that MoO_3 is dispersed over the surface, but slight diffusion into the lattice on calcination at elevated temperature cannot be ruled out. The surface species is rapidly reduced, while the bulk Mo^{+6} is reduced more slowly. At this stage, the formation of Mo(IV) takes over (see Fig. 5), resulting in an inflection point. The level of Mo(V), instead of continuously decreasing with time, reaches a plateau indicating the presence of a residual stable state. Reduction of Mo(V), an intermediate in the reduction path of Mo(VI) to Mo(IV), is enhanced by increasing the reduction temperature. So at 500 and 750°C, for a given period, less Mo(V) is formed, and the maximum shifted to shorter reduction time.

It is instructive to compare the conclusion reached here regarding the environment of Mo(V) with that of Mo(VI) obtained by a study of ir and uv reflectance spectra of unreduced MoO_3–Al_2O_3 and MoO_3-CoO–Al_2O_3. Lipsch and Schuit (*17*) have studied the ternary system both by ir and uv reflectance, while Ashley and Mitchell (*18*) have investigated the binary system, in addition to the ternary, by uv reflectance, with the general conclusion that Mo(VI) is both in tetrahedral and octahedral configuration. Our results indicate that at least the Mo(VI) which is reduced to Mo(V) and, observed by ESR, is in octahedral environment. On reduction, one oxygen atom is removed resulting in a tetragonal pyramidal environment for Mo(V), which satisfactorily explains the observed ESR spectrum.

CONCLUSIONS

The study reported here demonstrates that useful information on HDS catalysts can be obtained by studying the ESR spectra of Mo(V), particularly by measuring the absolute spin concentration of Mo(V) and by extracting appropriate information from the spectrum, which can be related to the environment of Mo(V). A study of reduction rates, by following the formation of Mo(V), suggests: (1) that Mo(V) is an intermediate in the reduction of Mo(VI) to lower valence states; (2) that there are two hexavalent species, one readily reduced and the other slowly reduced; and (3) the rate of formation of Mo(IV) is enhanced by increasing the reduction temperature. Structural differences between η- and γ-Al_2O_3 are reflected in the spectral parameters of Mo(V) signal and in supports in which the signal is observed at room temperature. Work is underway in which the effect of sulfiding and the presence of cobalt and nickel are studied.

ACKNOWLEDGMENT

The authors thank Mr. Arthur V. Fareri for his technical assistance in this work.

REFERENCES

1. *a.* Lipsch, J. M. J. G., and Schuit, G. C. A., *J. Catal.* **15**, 179 (1969) and references therein;
  b. Massoth, F. E., *J. Catal.* **30**, 204 (1973).
2. *a.* Seshadri, K. S., and Petrakis, L., *J. Phys. Chem.* **74**, 4102 (1970);
  b. Seshadri, K. S., Massoth, F. E., and Petrakis, L., *J. Catal.* **19**, 95 (1970);
  c. Mason, J., and Nechtschein, J., *Bull. Chem. Soc. Chim. Fr.* **10**, 3933 (1968).
3. *a.* Dalton, L. A., Bereman, R. D., and Brubaker, C. H., *Inorg. Chem.* **8**, 2477 (1969);
  b. Monoharan, P. T., and Rogers, M. T., *J. Chem. Phys.* **49**, 5510 (1968).
4. *a.* Nicula, A., Stamires, D., and Turkevich, J., *J. Chem. Phys.* **42**, 3684 (1965);
  b. Lumbeck, H., and Voitländer, J., *J. Catal.* **13**, 117 (1969).
5. Hyde, J. S., "Experimental Techniques in EPR," 6th Annual NMR-EPR Workshop, Nov. 5–9, Varian Associates Instrument Division, Palo Alto, CA (1962).
6. Hyde, J. S., and Brown, H. W., *J. Chem. Phys.* **37**, 368 (1962).
7. Naccache, C., Kodratoff, Y., Pink, R. C., and Imelik, B., *J. Chim. Phys.* **63**, 341 (1966).
8. MacIver, D. S., Wilmot, W. H., and Bridges, J. M., *J. Catal.* **3**, 502 (1964).
9. Dufaux, M., Che, M., and Naccache, C., *J. Chim. Phys.* **67**, 527 (1970).
10. Peacock, J. M., Sharp, M. J., Parker, A. J., Ashmore, P. G., and Hockey, J. A., *J. Catal.* **15**, 379 (1969).
11. Che, M., Vedrine, J., and Naccache, C., *J. Chim. Phys.* **66**, 579 (1969).
12. Lebedev, Ya. S., *Zh. Strukt. Khim.* **4**, 22 (1963).
13. Burlamacchi, L., Martini, G., and Ferroni, E., *Chim. Phys. Lett.* **9**, 420 (1971).
14. Kihlborg, L., *Acta Chem. Scand.* **13**, 954 (1959).
15. *a.* Kazanski, V. B., and Turkevich, J., *J. Catal.* **8**, 231 (1967);
  b. Berger, P. A., and Roth, J. F., *J. Phys. Chem.* **71**, 4307 (1967).
16. *a.* Yamaguchi, G., and Yanagida, H., *Bull. Chem. Soc. Japan* **35**, 1896 (1962);
  b. Yanagida, H., and Yamaguchi, G., *Bull. Chem. Soc. Japan* **37**, 1229 (1964).
17. Lipsch, J. M. J. G., and Schuit, G. C. A., *J. Catal.* **15**, 163 (1969).
18. Ashley, J. H., and Mitchell, P. C. H., *J. Chem. Soc. A*, 2730 (1969).